SLAC PUB-2338
May 1979
(I/A)

A Backscattered Laser Polarimeter for e^+e^- Storage Rings*

D. B. Gustavson, J. J. Murray, T. J. Phillips,
R. F. Schwitters†, C. K. Sinclair
Stanford Linear Accelerator Center, Stanford, CA 94305

J. R. Johnson, R. Prepost, D. E. Wiser
University of Wisconsin, Madison, WI 53706

ABSTRACT

This report describes the design, construction, and operation of a monitor of the transverse polarization of beams circulating in the Stanford Linear Accelerator Center e^+e^- storage ring SPEAR. This device measures an asymmetry in the Compton scattering of circularly polarized laser photons. Measurement of the beam polarization to a statistical precision of $\pm 5\%$ requires approximately two minutes under typical conditions.

(Submitted to Nuclear Instruments and Methods)

---

* Work supported by Department of Energy under contract numbers EY-76-C-03-0515 and EY-76-C-02-0881.

I. INTRODUCTION

Electron (positron) beams circulating in high energy storage rings may become transversely polarized anti-parallel (parallel) to the guide magnetic field by emission of synchrotron radiation with spin-flip[1]. In the absence of depolarizing effects, the polarization builds up in time according to:

$$P(t) = \frac{8\sqrt{3}}{15}\left(1 - e^{-t/T_{pol}}\right) \qquad (1)$$

$$T_{pol}(\text{sec}) = \frac{98.7\ r^3}{E^5}\frac{R}{r}$$

where r is the bending radius of the storage ring in meters, R is the mean radius, and E is the beam energy in GeV. Depolarization effects may substantially reduce the maximum achievable polarization of 92.4%. These effects are expected to be strongly energy dependent[2] and cannot in general be estimated with sufficient accuracy to obviate the need to monitor the beam polarization if it is of interest.

Various methods have been used to measure the beam polarization in e^+e^- storage rings. Touschek scattering has been the most widely applied technique. Briefly, Touschek scattering is intra-beam Møller scattering that leads to the correlated loss of pairs of particles from stable orbits due

to large exchange of laboratory frame energy. The Touschek scattering rate depends on beam polarization, allowing the polarization to be deduced from a measurement of the rate of correlated losses of particles from a single beam. This method has been applied with success at Novosibirsk[3], Orsay[4], and SPEAR[5]; details of the Touschek scattering technique can be found in Ref. 6. The second general method for measuring beam polarization has been the study of angular distributions of particles created in e^+e^- annihilation. These, again, depend in a well defined way on the degree of beam polarization. Such measurements have been performed at Novosibirsk[7] and SPEAR[8,9].

Both of these techniques have certain drawbacks that make it desirable to find other polarization monitoring methods. The Touschek method is subject to relatively low rates and large backgrounds, and it is difficult to determine the analyzing power with good precision. The measurement of angular distributions is subject to low data rates and requires off-line analysis. Furthermore, it is desirable to have an independent monitor so that the assumptions used in predicting the angular distributions of final state particles can be checked.

We have developed a rapid polarization monitor at the Stanford Linear Accelerator Center e^+e^- storage ring SPEAR, based on Compton scattering of circularly polarized photons from a laser. This method for measuring radiative polar-

ization of stored e^+e^- beams was first suggested by Baier and Khoze[10]. There have been many feasibility studies of this technique[11]; the works of Prescott[12] and Toner[13] were particularly useful to the conceptual design of this system. A schematic layout of the apparatus is shown in Fig. 1. Circularly polarized photons are focussed on the SPEAR positron beam. A detector measures the vertical angular distribution of the backscattered gamma rays. An up-down asymmetry in the backscattered gamma rate results if the positron beam is transversely polarized vertically.

The cross section for Compton scattering of circularly polarized photons on transversely polarized electrons or positrons can be written[14] in the laboratory frame as:

$$\frac{d^2\sigma}{d\rho\, d\phi} = \sigma_o \pm P_\gamma P_e \cos\phi\, \sigma_1 \qquad (2)$$

where ρ is the fraction of the maximum possible backscattered gamma ray energy, ϕ is the azimuthal angle of the backscattered gamma relative to the polarization direction of the electron or positron beam, P_γ is the magnitude of the circular polarization of the incident photon beam, and P_e is the transverse polarization of the electron beam. The + (-) sign is for left (right) handed circular polarization of the incident photon beam. The quantity ρ is given by:

$$\rho = k/k_{max} \qquad (3)$$

$$k_{max} = 4a\gamma^2\varepsilon_\gamma$$

$$a = (1 + \frac{4\gamma\varepsilon_\gamma}{m})^{-1}$$

where k is the energy of the backscattered gamma ray, γ is the Lorentz factor of the electron beam (E/m), and ε_γ is the incident photon energy. (We use a system of units in which $\hbar = c = 1$). The value of k_{max} ranges up to about 450 MeV at the highest SPEAR energies (around 3.7 GeV). The polar angle of the backscattered gamma ray in the laboratory is given by:

$$\theta \simeq \frac{1}{\gamma}\sqrt{(1-\rho)/a\rho} \tag{4}$$

and the cross sections σ_0 and σ_1 can be written:

$$\sigma_o = r_o^2 a\left\{\frac{\rho^2(1-a)^2}{1-\rho(1-a)} + 1 + \left[\frac{1-\rho(1+a)}{1-\rho(1-a)}\right]^2\right\}$$

$$\sigma_1 = r_o^2 a\left[\frac{\rho(1-a)}{1-\rho(1-a)}\right]\sqrt{4a\rho(1-\rho)} \tag{5}$$

where r_0 is the classical electron radius.

It is evident from the preceding equations that the maximum beam polarization information occurs for backscattered gamma rays of relatively high energy. The polar angles of these gamma rays are of order $1/\sqrt{3}\,\gamma$, a very small

angle at the beam energies of interest. These small angles pose two problems for a polarization monitor. First, the angular resolution of the detector must be fine enough so that the $\cos\phi$ term of Eq. (2) can be resolved. Second, the angular divergence of the electron or positron beam must be small compared to typical backscattered gamma ray angles or else the polarization information will be lost.

In general, particles moving in e^+e^- storage rings are distributed in transverse phase space with density contours defined by the ellipses:

$$\gamma y^2 + 2\alpha yy' + \beta y'^2 = \varepsilon \qquad (6)$$

where y represents the horizontal or vertical position relative to the equilibrium orbit and y' is the corresponding angle. The beam emittance is represented by ε and may be different for vertical and horizontal motion. Here α, β, γ are characteristic functions of the storage ring. They are periodic and may differ for vertical and horizontal motion. They are related to each other by:

$$\gamma = \frac{1 + \alpha^2}{\beta} \qquad \alpha = -\tfrac{1}{2}\beta' \qquad (7)$$

where β' represents the derivative of the β-function with respect to position along the orbit. Assuming the incident photons interact with the electron or positron beam over a

small enough region that α, β, γ do not vary significantly, the projected spot size of the beam on a target a distance L away from the intersection point is:

$$\Delta y = \sqrt{\varepsilon(\beta - 2\alpha L + \gamma L^2)} \quad . \tag{8}$$

If the detector has a RMS position resolution Δ and the RMS beam size at the interaction point is Σ, then the net angular resolution of the system δ is given by:

$$\delta = \left\{ \left(\frac{\Sigma}{\beta}\right)^2 \left[1 + (\alpha - \beta/L)^2\right] + \frac{\Delta^2}{L^2} \right\}^{\frac{1}{2}} \quad . \tag{9}$$

In order to achieve acceptable analyzing power (measured asymmetry for 100% beam polarization), it is necessary to find a set of parameters for Eq. (9) such that $\gamma\delta < 1$. The angular resolution is optimized by making L as large as possible subject to the condition

$$\alpha = \beta/L \quad . \tag{10}$$

If the measurement error Δ can be neglected, then Eq. (10) can be used to find an appropriate L given α and β. Because Σ^2/β is an invariant, the angular resolution is optimized by choosing an intersection point where the β-function is at or near its maximum value.

Restrictions on possible locations in the SPEAR lattice and the beam optics considerations discussed above allow for one intersection point with the positron beam in a short straight section between two bending magnets. In the case of SPEAR, the horizontal emittance is large enough to destroy the polarization information in that component and only the vertical profile of the backscattered gamma rays is measured. The vertical β- and α- functions at the chosen intersection point are 20 m and 1.5, respectively, and L was chosen to be 13 m. Assuming a detector resolution of 200 μm, the product $\gamma\delta$ for the SPEAR polarimeter is approximately 1/3 at a beam energy of 4 GeV, and smaller at lower energies. The projected spot size in the horizontal direction at the detector is approximately 15 mm FWHM at 4 GeV.

The expected vertical distribution of backscattered gamma rays at the detector is obtained from the preceding cross section formulae by integrating over the horizontal position, smearing by the angular divergence of the incident beam, and taking into account the low gamma ray energy cut-off of the detector. The vertical distribution can be written (assuming $P_\gamma = 1$):

$$\frac{d\sigma}{dy} = \frac{d\sigma_o}{dy} \pm P_e \frac{d\sigma_1}{dy} \qquad (11)$$

where, again, the + (-) refers to left (right) circular polarization. Representative values of $d\sigma_{0,1}/dy$ are shown in Fig. 2.

To determine P_e, an up-down asymmetry is formed using the number of events in bins on the sides of the vertical distribution. To cancel false asymmetries, the up-down asymmetries for both left and right circular polarizations are averaged (with opposite sign). The mean up-down asymmetry A is related to P_e by:

$$A = \Pi P_e \tag{12}$$

where the analyzing power Π is given by:

$$\Pi = \int_{\Delta y} dy \frac{d\sigma_1}{dy} \Big/ \int_{\Delta y} dy \frac{d\sigma_o}{dy} \quad . \tag{13}$$

Here Δy represents the bins used in the asymmetry measurement. The predicted analyzing power for the SPEAR polarimeter is shown in Fig. 3.

For access reasons, the incident laser photon beam was focussed on the positron beam with a vertical crossing angle δ_ℓ of 8 mrad and with zero horizontal crossing angle. The positrons are compressed in a bunch less than 0.5 nsec long that circulates around SPEAR at a frequency f_0 = 1.28 MHz.

The laser is pulsed in synchronism with the rotation of the positron bunch; its pulse width is large compared to the positron bunch length. The laser spot size is small compared to the positron beam width. Under these conditions, the luminosity (counting rate per unit cross section) can be written as:

$$\mathcal{L} = \frac{2\,\tilde{P}\,i_b}{\sqrt{2\pi}\,cf_o e^2 \varepsilon_\gamma \delta_\ell \Sigma_x}\,\mathrm{Erf}\left(\frac{\ell\,\delta_\ell}{2\sqrt{2}\,\Sigma_y}\right) \tag{14}$$

where $\tilde{P}$ is the peak laser power, i_b is the circulating e^+ beam current, Σx and Σy are the RMS beam sizes of the e^+ beam in the horizontal and vertical planes, respectively, and ℓ is the length over which the beams interact. The Erf-function is approximately unity.

II. APPARATUS

A. Laser and Optics

A cavity-dumped Argon-ion laser[15] generating the 514.5 nm (2.41 eV) line is used for the measurements. The cavity-dumped pulses are delivered at the beam circulation frequency of SPEAR, initiated by a signal derived from the storage ring radio frequency to ensure that the optical and positron beam pulses overlap stably in time. Each optical pulse has a width of approximately 12-15 nsec and a peak power of up to 80 watts. A fast photodiode is provided to check the laser output pulse shape. Fig. 4 shows a typical oscilloscope trace of the photodiode response.

The laser light is vertically polarized by Brewster angle windows on its plasma tube. Conversion to either right or left circularly polarized light is accomplished with a cylindrical ring electrode KD*P Pockels cell[16]. The cell is driven to either positive or negative quarter wave phase shift by a solid state square wave pulser of variable period. The transition time between the two polarization states is deliberately kept rather long to suppress acoustic and/or piezo-electric oscillations in the cell. In practice, the polarization is switched between left circular and right circular at about 20 Hz. A gating system assures

that data are not recorded during the transition periods. The optical axis of the Pockels cell was aligned parallel to the laser beam by observing the interference pattern produced with the Pockels cell between crossed polarizers.

The circularly polarized laser beam passes through a simple lens, used as both a steering and focussing element, and enters the storage ring vacuum through a type 7056 glass window mounted on a mini-conflat flange. The window was carefully annealed, and studied with a Babinet-Soleil compensator to assure that it did not have any significant optical retardation.

B. Beam Line

A plan view of the experimental layout is shown in Fig. 5. The laser beam is aimed at the interaction point from above, at an angle of 8 mrad to the plane of the storage ring. This angle provides the required separation between incident and backscattered beam lines, allowing about 10 cm clearance at the position of the gamma ray detector. The rough alignment of the laser beam is performed with the aid of two optical targets, which were surveyed accurately and may be inserted to a precise location under remote control. Each target consists of a quadrant photodetector which gives the same output on each quadrant when the incident laser

beam is centered. Fine steering adjustments are made by translating the remotely movable lens located midway between the laser and the interaction point.

The laser beam enters the SPEAR vacuum through a window on the end of a vacuum chamber extension of sufficient length to bring the window outside the SPEAR bending magnet nearest the interaction point. This extension is part of a modified vacuum chamber which also includes a reduced amount of aluminum (2 cm thickness) along the path of the backscattered gamma rays. This aluminum serves as a partial filter to reduce the background from synchrotron radiation. Additional filtering is provided by a 1.8 mm thickness of niobium placed in the backscattered beam line near the exit from the SPEAR vacuum chamber. This absorber was selected to reduce the synchrotron radiation leakage to a negligible level in a minimum number of radiation lengths.

Since the optimum position for the backscattered gamma detector places it outside the SPEAR shielding tunnel, a penetration was provided in the shielding wall. This also allows the laser to be mounted outside the tunnel for easy access and adjustment. The penetration contains a collimator with a thickness of 20 cm of lead and 30 cm of paraffin, with holes for both incident laser photons and backscattered gamma rays. Remotely moveable lead beam stoppers are located at each end of the penetration. A steel box surrounding the laser and detector is interlocked

so that access is possible only when these stoppers are in. As a further safety measure, aluminum boxes and beam tubes surround the laser beam line to prevent inadvertent exposure to the intense laser light.

C. Detector

Fig. 6 is a diagram of the detector arrangement used to measure the vertical distribution of the backscattered gamma rays. The basic photon trigger is provided by a telescope of 3 small scintillation counters, labeled S1, S2, and S3. S1, with an active area of 7.6 cm x 7.6 cm, serves to veto charged particles. S2 and S3, each 2.5 cm high x 4.1 cm wide, follow a 1/2 radiation length tungsten converter plate and are used in coincidence to trigger on electron-positron pairs produced in the converter. The energy of a pair, and thus of the incident photon, is measured by the pulse height from a sodium iodide crystal placed behind the trigger counters. The crystal is a 7.6 cm diameter by 15.2 cm long cylinder and is viewed by an Amperex 56DVP photomultiplier tube.

The vertical position of a converted photon is determined from the drift time of ionization produced in a single-cell drift chamber (2.5 cm x 5 cm active area) placed immediately behind the converter. The vertical drift field

is produced by 10 pairs of field wires which are spaced 2.54 mm apart, with a gap of 6.35 mm between members of a pair. The signal is collected on a single sense wire in the center of a 5.6 mm ID nickel-plated brass tube which has a slot opening into the drift region. The sense wire is read out at ground potential, and a negative high voltage is applied to a resistor chain to distribute the required potentials to the field wire pairs and to the tube surrounding the sense wire. In practice, about -3500V is required for efficient operation. The chamber is filled with a gas mixture of 50% Argon, 50% Ethane at atmospheric pressure. Laboratory tests of this chamber with a collimated source showed very linear response of drift time versus source position with a drift velocity of about 50 μm/nsec. The resolution is limited by the 4 nsec bin size accepted by the electronics.

In the early stages of running, the backscattered photon detector system consisted of two small multi-wire proportional chambers separated by a converter plate. The first chamber had 2 mm wire spacing with wires oriented vertically and could be used as a charged particle veto and to monitor the horizontal alignment of the detector with respect to the beam line. The second chamber, following the converter, had 1 mm wire spacing with wires oriented horizontally and served to measure the vertical distribution of the backscattered beam in 1 mm bins. This detector arrangement was replaced by the drift chamber system

described above, to allow finer bin size on the vertical profile measurements along with more powerful computer analysis.

D. Logic and Computer

Fig. 7 shows a diagram of the data acquisition system. The drift time is digitized by the TDC feature of an analyzer with four selectable memory regions[17]. The start pulse is obtained from the basic $\overline{S1}\cdot S2\cdot S3$ photon trigger with a cut on photon energy from the sodium iodide crystal. The stop pulse comes from either the drift chamber pulse or a delayed signal derived from the SPEAR RF. This ensures a stop pulse in the event that the drift cell does not fire. The events are accumulated in two different regions of the analyzer memory, selected according to the photon polarization state as determined by the Pockels cell controller.

Initially, a small microcomputer was provided for data handling and run control. The system used a chassis and CPU built around a 4 MHz microprocessor[18] and the S-100 bus. To this was added 8K bytes of EPROM (erasable/programmable read only memory), 48K bytes of RAM (random access memory), and a video display driver, all commercially available. In addition, circuits were designed and built to provide

interfaces to CAMAC, a keyboard and 55 character/second printer[19], and a 2400 baud link to the SLAC Triplex computer system. A similar system has been described in more detail elsewhere[20].

The microcomputer system was programmed in assembly language to perform tasks such as the following:

-- start and stop runs, of preset length in time or scaled counts if desired; succeeding runs could be started automatically.

-- accept and analyze individual events through CAMAC at a rate of several KHz.

-- accept and analyze data acquired by the drift chamber system, accumulated over a period of several minutes at rates up to about 20 KHz.

-- gate the laser on or off, allowing measurements of both signal and background for each run.

-- at the end of a run, print out scaler data and/or histograms of events, and calculate quantities such as corrected asymmetries, errors, and elapsed time.

-- transmit asymmetries and/or histograms to the SLAC Triplex computer system for storage and later analysis.

After roughly a year of operation, the polarimeter software was transferred to the Sigma 5 computer that controls SPEAR operation. This system includes a teletype, a rack mounted display scope, a rack mounted panel with

input switches for program control, and a Branch Driver/ Branch Receiver combination for driving the 50 m cable from the SPEAR control room to the polarimeter CAMAC crate. The advantages gained in switching to the Sigma 5 include: availability of Fortran; access to more powerful software on the Sigma 5; accessability of the control station to other experimenters and machine operators interested in monitoring the polarization; and the ability to pass asymmetry measurements to a common area in the computer so the operators and experimenters have access to it directly through their software.

III. POLARIMETER OPERATION

A. System Alignment

The alignment procedure for the polarimeter consists of finding optimum overlap of the laser and positron beams in both space and time. The first step is the alignment of the laser beam with respect to the optical targets described in Section II. These targets are inserted remotely into fixed locations along the expected laser beam line, and the laser bench is adjusted so that the beam is centered on both targets. The remotely movable focussing lens is then inserted and positioned so that the beam is again centered on the downstream laser target. The optical targets are then withdrawn from the beam line. This preliminary alignment is sufficient to give some backscattered rate.

The final alignment of the optical system is achieved by maximizing the backscattered Compton rate. The timing of the laser pulse is set with respect to the positron bunch by varying the delay of the pulse that is used to trigger the laser cavity dumper and monitoring the backscattered $\overline{S1}\cdot S2\cdot S3$ rate. The final laser beam steering is then accomplished by translating the lens. The backscattered $\overline{S1}\cdot S2\cdot S3$ rate is optimized with respect to both a vertical and a horizontal scan of the lens position. A typical

horizontal scan is shown in Fig. 8. The measured horizontal beam size as determined by the scan is consistent with the expected beam size at that energy and has a full width at half maximum of approximately 2 mm at a beam energy of E = 1.78 GeV.

B. Detection of the Backscattered Gamma Rays

The vertical profile of the backscattered distribution is measured with the detector system described in Section II. For most of the data taking, the gamma ray energy threshold was set to exclude approximately the lower 10% of the backscattered energy spectrum, since that region contributes very little polarization information.

The measured backscattered rates typically range from about 1340/mA-W-sec (1340 events per second for 1 Watt of average laser power and 1 mA of stored positron current) at 3.7 GeV to about 1750/mA-W-sec at 1.88 GeV, the change with energy resulting primarily from the linear dependence of the beam size on beam energy. With typical running conditions of average laser power P=0.50 Watt and positron stored beam current i_b=20mA, the backscattered rates are typically 13-18 kHz. The laser-off contribution is quite small, ranging from 0.5% to 2.5% of the laser-on rate. The event rate accepted under the above conditions is typically 90% of the

trigger rate, with the inefficiency set by the dead time of the TDC unit used to perform the time measurements. Expressions are given in Section I for the Compton cross section and the expected luminosity in terms of laser and positron beam parameters. The measured rates are in satisfactory agreement with those calculated.

The measured vertical profile of the backscattered gamma rays depends upon the Compton effect angular distribution, the positron beam vertical emittance, and the detector resolution and location. The dominant factors for the conditions of these measurements are the Compton angular distribution and the detector distance from the interaction point. Typical vertical profiles measured with the drift chamber are shown in Fig. 9(a) and 10(a) for beam energies of 2.05 and 3.60 GeV respectively.

3. Pockels Cell

The linearly polarized light produced by the laser is converted to circular polarization by a Pockels cell placed directly downstream of the laser. The circular polarization is switched from left to right at a frequency of about 20 Hz by switching the voltages on the Pockels cell. However, before serious data taking, the voltage settings of the Pockels cell must be empirically checked to determine that

(a) maximal left and right circular polarization are obtained, and (b) false asymmetry effects due to residual linear polarization are minimized.

Preliminary voltage settings were determined with the aid of a Babinet-Soleil compensator. Using these settings as starting values, the detector is operated with the beam at an energy known to yield zero polarization. Defining $V_\Sigma = V_+ + V_-$ and $V_\Delta = V_+ - V_-$, where V_+ and V_- are the Pockels cell voltages which nominally yield right and left circular polarization, the final settings of the cell voltages are then obtained by varying V_Σ and V_Δ while accumulating vertical profile data for the two polarization states. The difference between the two profiles is made zero by an appropriate choice of V_Δ, and V_Σ is later chosen to optimize the observed asymmetry on a genuine polarization signal.

D. Asymmetry Measurements

As shown in Section I, a non-zero positron beam polarization results in an up-down asymmetry in the backscattered gamma ray vertical distribution. During a data run, vertical distributions are accumulated separately for right and left circular polarization settings of the Pockels cell. An individual run lasts typically 2-3

minutes, preceded and followed by 10 sec laser-off runs. With ~15 kHz backscattered rates, approximately 10^6 events are normally accumulated in each distribution. The actual width of the distribution is dependent on the beam energy. The difference between distributions for left and right circular polarization is shown in Fig. 9(b) for an unpolarized positron beam at an energy of 2.05 GeV, and in Fig. 10(b) for a polarized beam at 3.60 GeV.

The experimental asymmetry A_{exp} is obtained online by the following procedure:

a. The left (L) and right (R) distributions are added together and the most probable bin is determined.

b. Individual up-down asymmetries are calculated, defined as

$$\left.\frac{U-D}{U+D}\right|_{L,R} = A_{L,R}$$

where U,D refer to sets of bins above and below the most probable bin, and are chosen to maximize the statistical precision of the measurement. The experimental asymmetry is then defined as $A_{exp} = \frac{A_L - A_R}{2}$. This combination eliminates false aysmmetries due to inexact centering of the U,D regions or other systematic effects.

A 3 minute run typically yields a value of A_{exp} with a statistical error of $\pm 0.1\%$.

IV. RESULTS

Fig. 11 shows an example of asymmetry measurements as a function of time during a single SPEAR fill. Here the elapsed time was defined to start from zero when the storage ring had finished ramping to its final energy of 3.7 GeV. The solid curve is a fit to the expected time dependence of the beam polarization expressed by Eq. (1). Similar measurements and fits have been made at other energies where there was expected to be little depolarization. For each energy, the time constant T_{pol} may be obtained from the fit. Fig. 12 shows fitted time constants for polarization build-up at 2.82, 3.26 and 3.70 GeV. The solid line represents the theoretical expression from Eq. (1). The agreement is excellent.

In the absence of significant depolarizing effects, Eq. (1) indicates the beam polarization is expected to approach an asymptotic value of $8\sqrt{3}/15 = 0.924$. In the region of beam energies near 3.7 GeV, T_{pol} is sufficiently small (~15 minutes) that a very nearly asymptotic value of the experimental asymmetry may be reached in a reasonable time. The maximum value achieved has been found to be approximately 2.6%, in satisfactory agreement with the calculated analyzing power shown in Fig. 3. The fitted asymptotic values at lower energies are also consistent with

the calculation.

Since calculations of depolarizing effects indicate strong energy dependence, including both broad and narrow resonances, it is of interest to study changes in beam polarization as a function of machine energy. A series of asymmetry measurements can be made while the SPEAR energy is raised in small steps, remaining at each energy long enough to allow a good determination of any change in the asymptotic asymmetry. Fig. 13 shows the results of such a scan, covering SPEAR energies from about 3.60 to 3.66 GeV in 10 MeV steps. The measured asymmetry builds from zero at the beginning of the fill, but tends towards a different asymptotic value for each energy value.

In general, during any one of the fixed energy segments of such a scan the asymmetry is expected to vary with time according to

$$A(t) = \frac{A_f}{1+x} + \left[A_i - \frac{A_f}{1+x} \right] e^{-t(1+x)/T_{pol}} \qquad (15)$$

Here A_i is the asymmetry at the beginning of the segment, A_f represents the asymptotic asymmetry in the case of no depolarization, and the quantity x is defined as $x = \frac{T_{pol}}{T_{depol}}$ where T_{depol} is the depolarization time constant. Fits of this function for A_i, A_f, and x have been made to scans such as that shown, with x constrained to be positive and the entire curve required to be piecewise continuous. The value

of A_f is required to be the same for all segments, and T_{pol} is calculated for each energy using Eq. (1). The results of such a fit are shown as the solid curve in Fig. 13. The fitted x values for this scan are plotted in Fig. 14, along with the results of an absolute theoretical calculation[21]. The agreement is quite good.

The measurements presented above were obtained with a single beam of positrons in the storage ring. As indicated by the comparisons shown, the general features of the single-beam results obtained are in good agreement with theoretical expectations. Measurements with colliding beams have exhibited the expected tune shifts and broadening of single-beam resonances, but have also shown strong depolarization behavior that is not currently understood. Detailed studies of single beam and colliding beam depolarization are continuing and will be reported elsewhere.

The authors would like to acknowledge the help of G. E. Fischer in the initial stages of this project, and the important contributions of R. Eisele, A. Gallagher, and J. Jurow in the design and implementation of the necessary changes in the SPEAR storage ring. M. Browne, J. Escalera, K. Jobe, M. Lateur, C. Noyer, and E. Taylor provided technical support for instrumentation and installation of experimental apparatus and beam lines. This work was supported by the Department of Energy under contract numbers EY-76-C-03-0515 and EY-76-C-02-0881.

REFERENCES

† Permanent Address: Physics Department, Harvard University, Cambridge, MA 02138.

1. A. Ā. Sokolov and I. M. Ternov, Sov. Phys.-Dokl. 8, 1203, (1964). J. D. Jackson, Rev. Mod. Phys. 48, 417 (1976).

2. Ya. S. Derbenev and A. M. Kondratenko, Sov. Phys.-JETP 35, 280 (1972). Ya. S. Derbenev and A. M. Kondratenko, Sov. Phys.-JETP 37, 968 (1973).

3. V. N. Baier, Sov. Phys.-Usp. 14, 695 (1972). S. I. Serednyakov, et al., Sov. Phys.-JETP 44, 1063 (1976).

4. D. Potaux, Proc. of the 8th Int. Conf. on High Energy Accelerators, CERN, 1971, p. 127, edited by M. H. Blewett, European Organization for Nuclear Research, Geneva.

5. U. Camerini, et al., Phys. Rev. D12, 1855 (1975).

6. W. T. Ford, A. K. Mann, and T. Y. Ling, SLAC Report No. 158 (1972).

7. L. M. Kurdadze et al., Novosibirsk Preprint No. 75-66 (1975). Ya. S. Derbenev et al., Particle Accelerators 8, 115 (1978).

8. J. G. Learned, L. K. Resvanis, and C. M. Spencer, Phys. Rev. Lett. 35, 1688 (1975).

9. R. F. Schwitters, et al. , Phys. Rev. Lett. 35, 1320 (1975).

10. V. N. Baier and V. A. Khoze, Sov. J. Nucl. Phys. 9, 238 (1969). It has long been recognized that the spin dependence of Compton scattering is useful for analyzing the polarization of free electrons. For examples, see the review article of L. A. Page, Rev. Mod. Phys. 31, 759 (1959).

11. See for example, Proc. of the 1974 Summer Study, SLAC/LBL Report No. PEP-137, (1974).

12. C. Prescott, SLAC TN-73-1 (1973).

13. W. T. Toner, SLAC/LBL Report No. PEP-172, op. cit. ref. 11.

14. F. Lipps and H. A. Tolhoek, Physica 20, 85 and 395

(1954).

15. The laser is a Spectra-Physics Model 166-09 equipped with a Model 365 acousto-optic Cavity Dumper.

16. The Pockels cell is a Lasermetrics Model 1043 with wedged crystal and windows, AR coating, and fluid filling.

17. The analyzer is a LeCroy Research Systems Model 3001 qVt.

18. The chassis and CPU board are a Z2 computer system from Cromemco, which incorporates a Zilog Z80A microprocessor.

19. The printer is a Qume model S3/55.

20. D. B. Gustavson and K. Rich, IEEE Trans. Nucl. Sci. NS-25, 226 (1978).

21. A. W. Chao, SLAC/LBL Report No. PEP-257 (1977).

FIGURE CAPTIONS

1. Schematic layout of apparatus. Open arrows indicate polarization states.

2. Calculated values of (a) $d\sigma_1/dy$ and (b) $d\sigma_0/dy$ (see Eq. (11)) for the SPEAR polarimeter setup with E = 3.7 GeV.

3. Calculated analyzing power for the SPEAR polarimeter as a function of beam energy for two strategies for calculating up-down asymmetries. Solid curve is the strategy used in practice; it assumes fixed bins Δy for all energies. Dashed curve assumes bin sizes and positions that scale with beam energy as 1/E.

4. Cavity-dumped laser output pulse shape measured with a fast photodiode.

5. Plan view of the experimental layout (a) outside and (b) inside the SPEAR shielding tunnel.

6. Schematic elevation view of the drift chamber detector arrangement. S1, S2, S3 are trigger scintillators and the small drift cell is labeled DC.

7. Logic diagram of the data acquisition system.

8. Backscattered gamma rate as a function of horizontal laser beam position at the point of interaction with the SPEAR positron beam, at an energy of 1.78 GeV. The solid line is a hand-drawn curve.

9. (a) Sum of and (b) difference between measured vertical distributions of backscattered gamma rays for right and left circularly polarized incident photons for an unpolarized positron beam at an energy of 2.05 GeV. The experimental asymmetry as defined in Section III.D is $(-.087 \pm .096)$ %.

10. (a) Sum and (b) difference distributions for a polarized positron beam at 3.60 GeV. The resulting value of A_{exp} is $(2.55 \pm .14)$ %.

11. Measured asymmetry versus time with 3.7 GeV positrons in SPEAR.

12. Polarization time constant versus energy. The data points are the results of fits to the observed build-up of asymmetry at 3 energies. The solid line is the theoretically expected behavior.

13. Asymmetry measurements versus time, for approximately 10 MeV steps of SPEAR energy in the region of 3.60 to 3.66 GeV. The solid line is a fit to Eq. (15).

14. Results from the fit shown in Fig. 13. The solid line is from an absolute theoretical calculation by Chao[18].

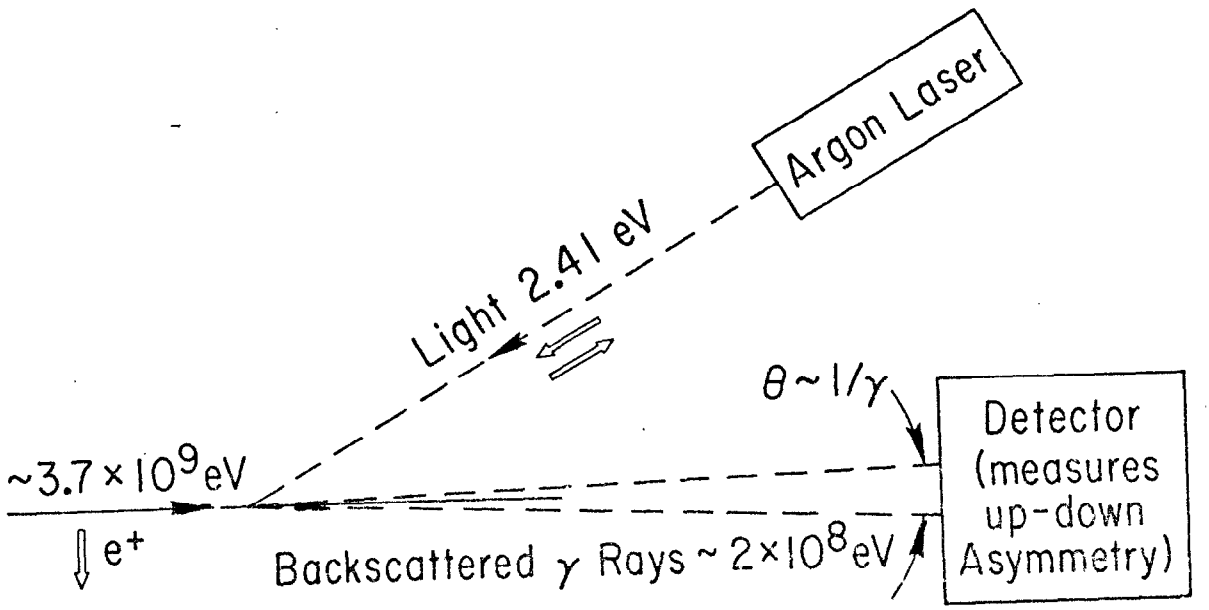
Argon Laser
Light 2.41 eV
θ~1/γ
Detector
(measures
up-down
Asymmetry)
~3.7×10^9eV
e+
Backscattered γ Rays ~ 2×10^8eV
3384A2
4-78

Fig. 1

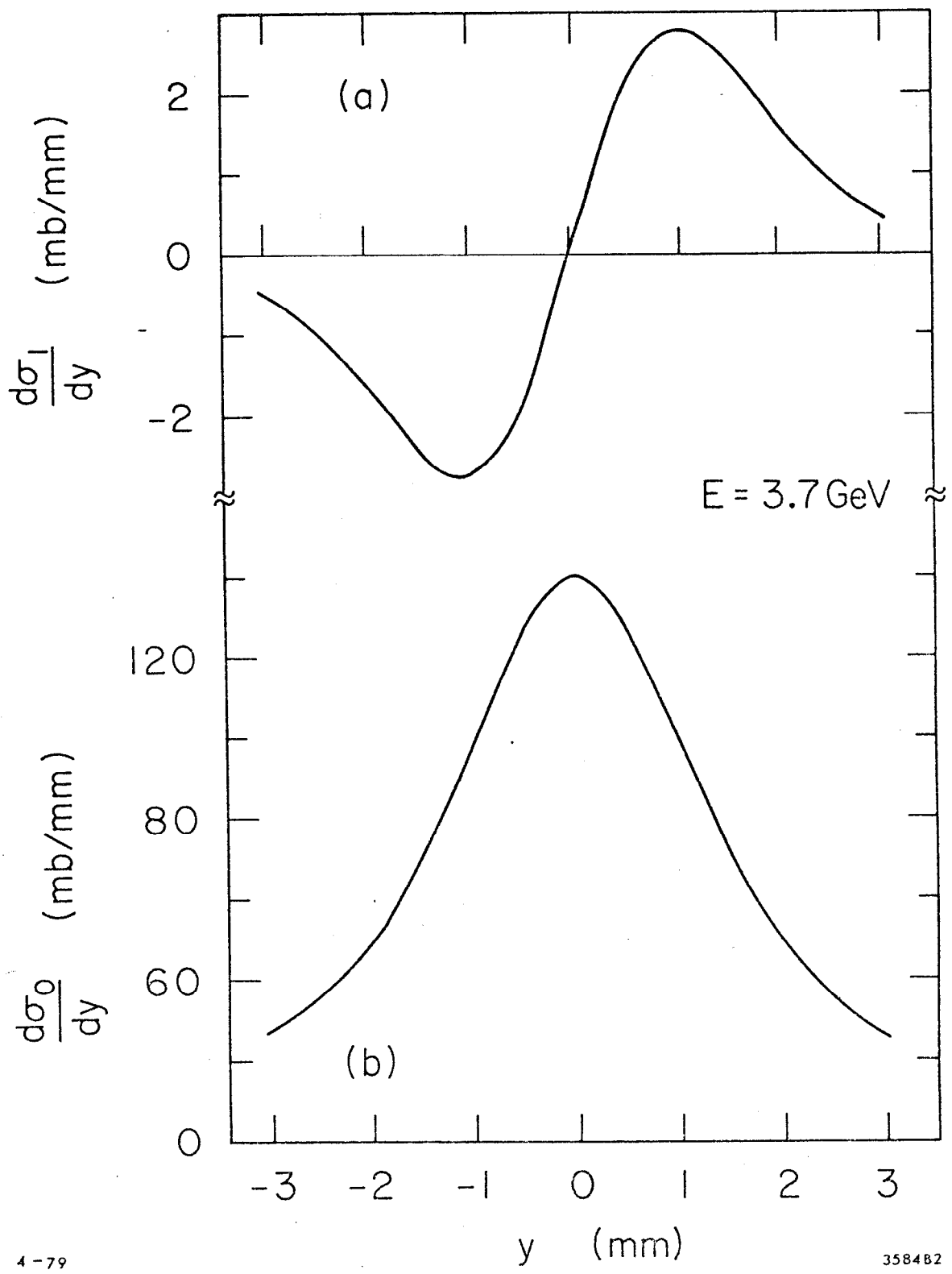
(a)
2
0
-2
$\frac{d\sigma_1}{dy}$ (mb/mm)
E = 3.7 GeV
120
80
60
0
(b)
$\frac{d\sigma_0}{dy}$ (mb/mm)
-3
-2
-1
0
1
2
3
y (mm)
4-79
3584B2

Fig. 2

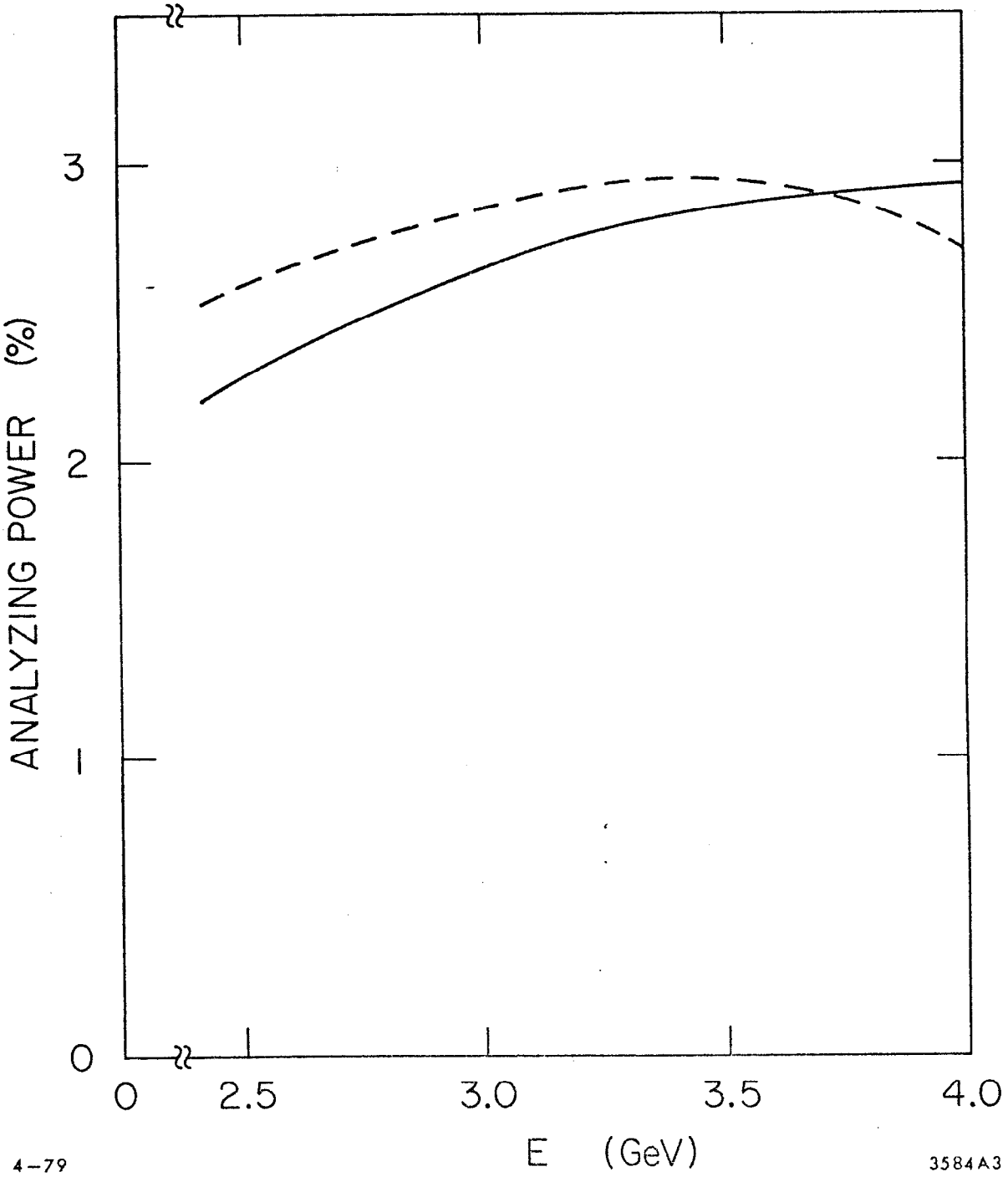

Fig. 3

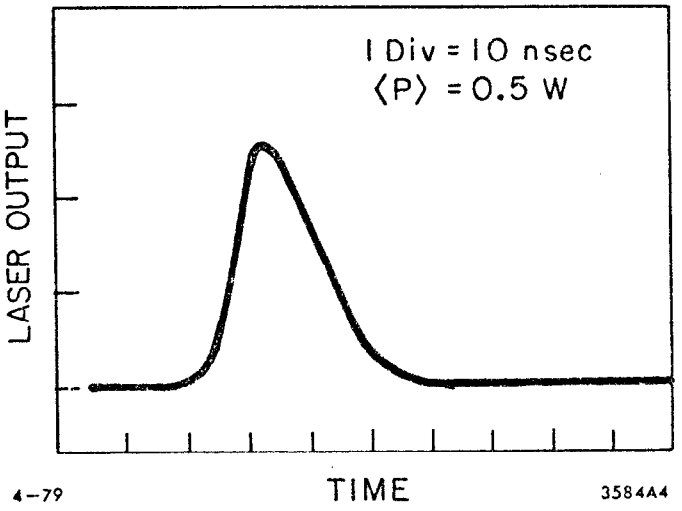

Fig. 4

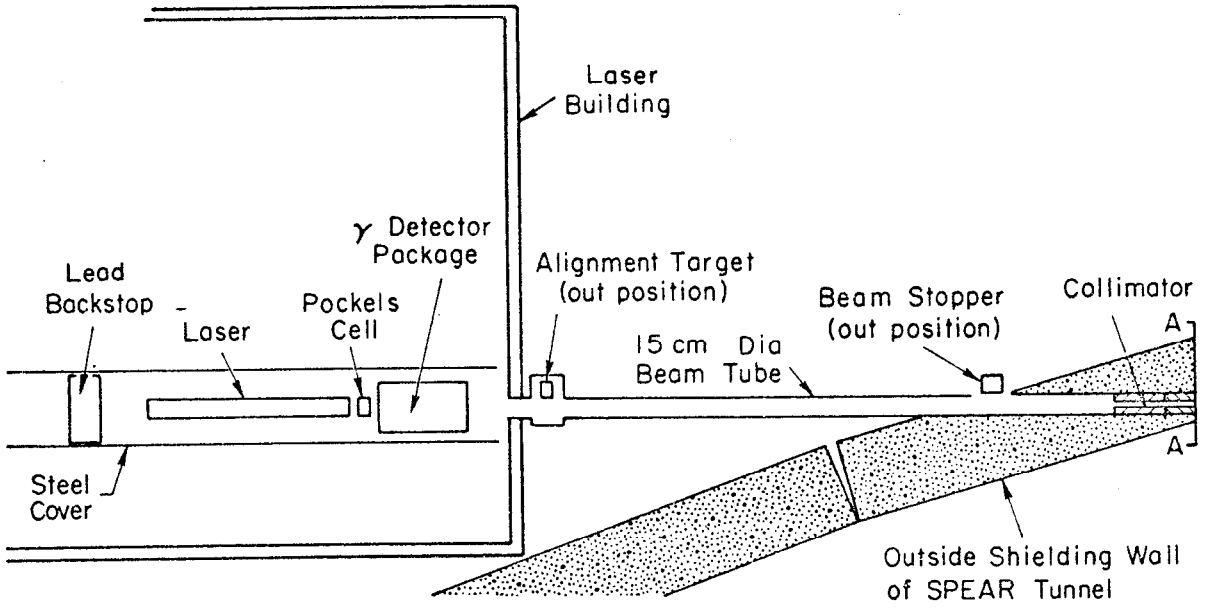

(a)

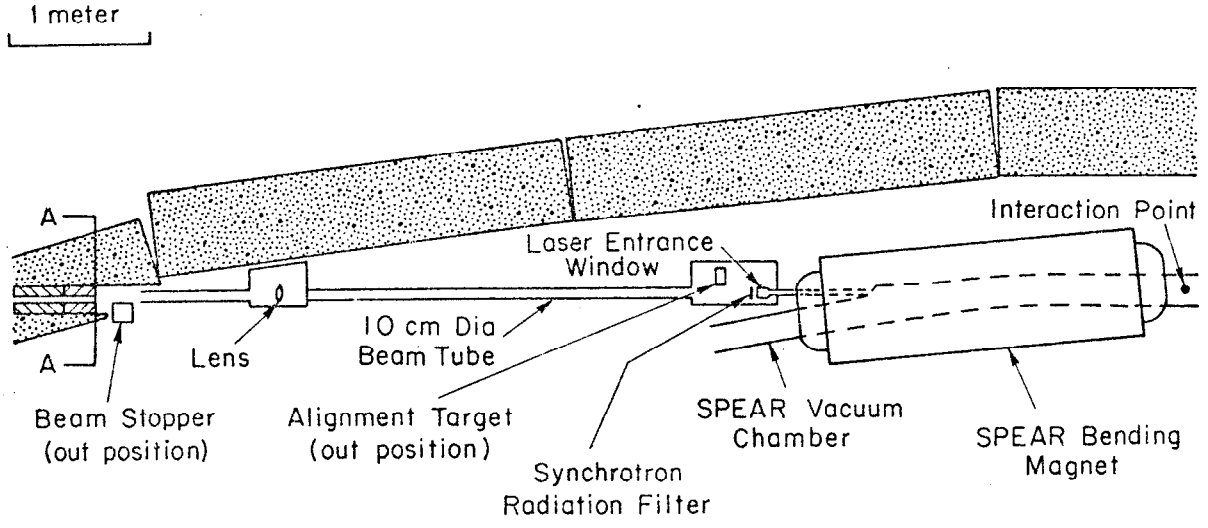

(b)

4-79

3584B1

Fig. 5

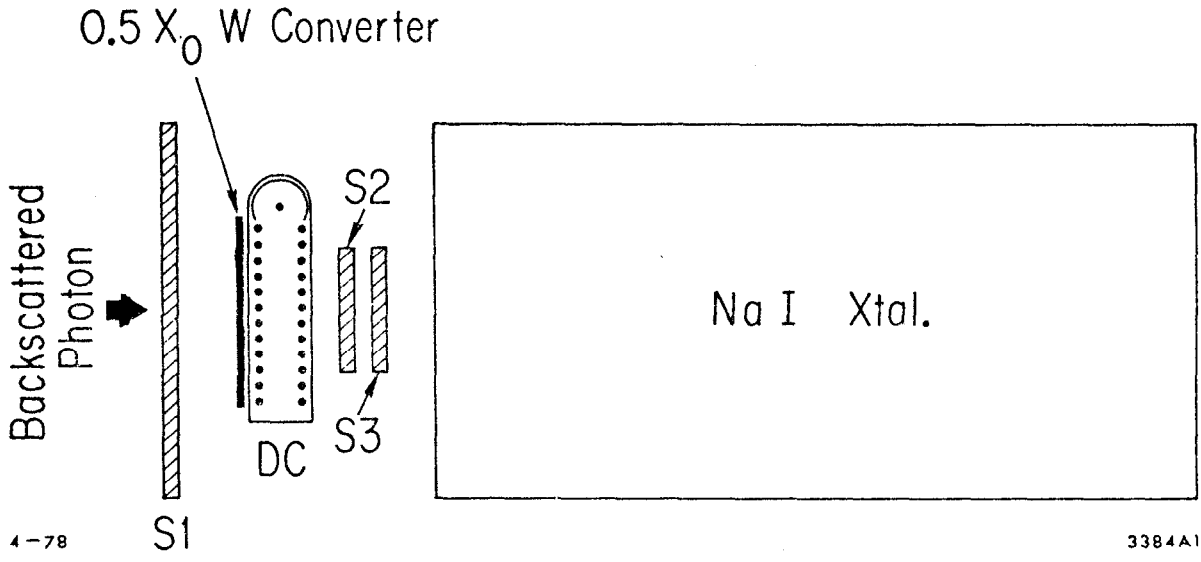
0.5 X0 W Converter
Backscattered Photon
S1
DC
S2
S3
Na I Xtal.
4-78
3384A1

Fig. 6

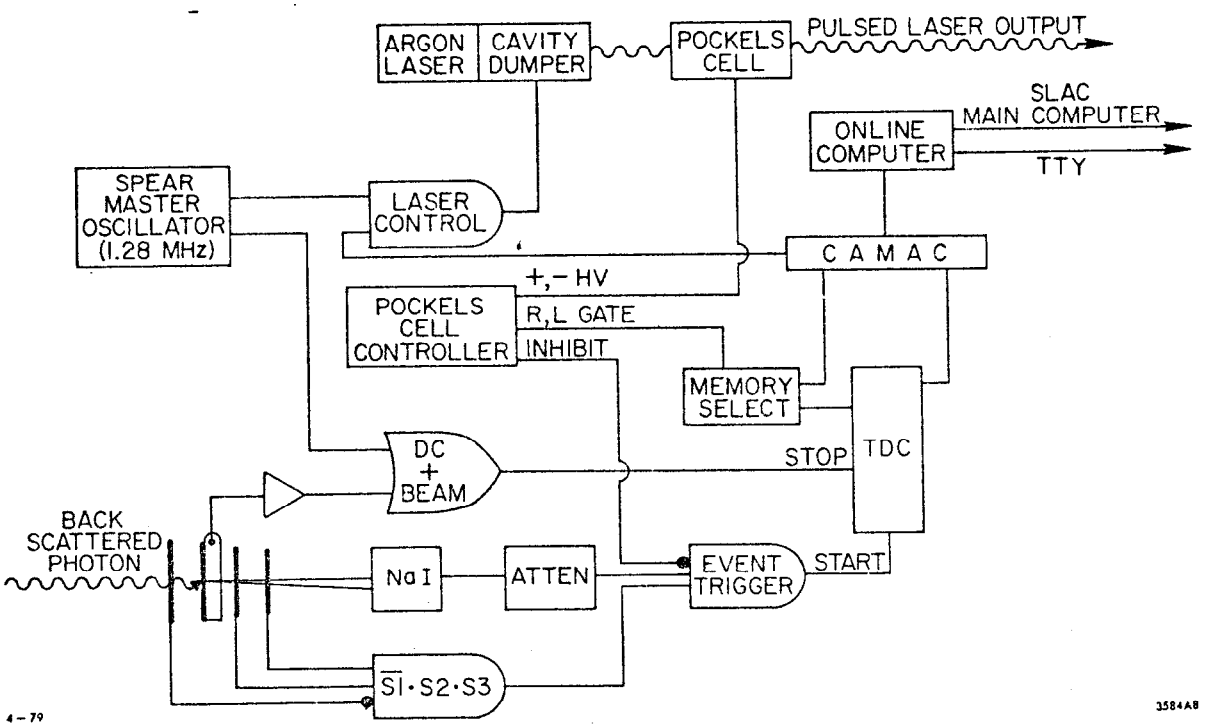
ARGON LASER
CAVITY DUMPER
POCKELS CELL
PULSED LASER OUTPUT
SLAC MAIN COMPUTER
ONLINE COMPUTER
TTY
SPEAR MASTER OSCILLATOR (1.28 MHz)
LASER CONTROL
C A M A C
+,- HV
POCKELS CELL CONTROLLER
R,L GATE
INHIBIT
MEMORY SELECT
TDC
DC + BEAM
STOP
BACK SCATTERED PHOTON
NaI
ATTEN
EVENT TRIGGER
START
S1·S2·S3
4-79
3584A8

Fig. 7

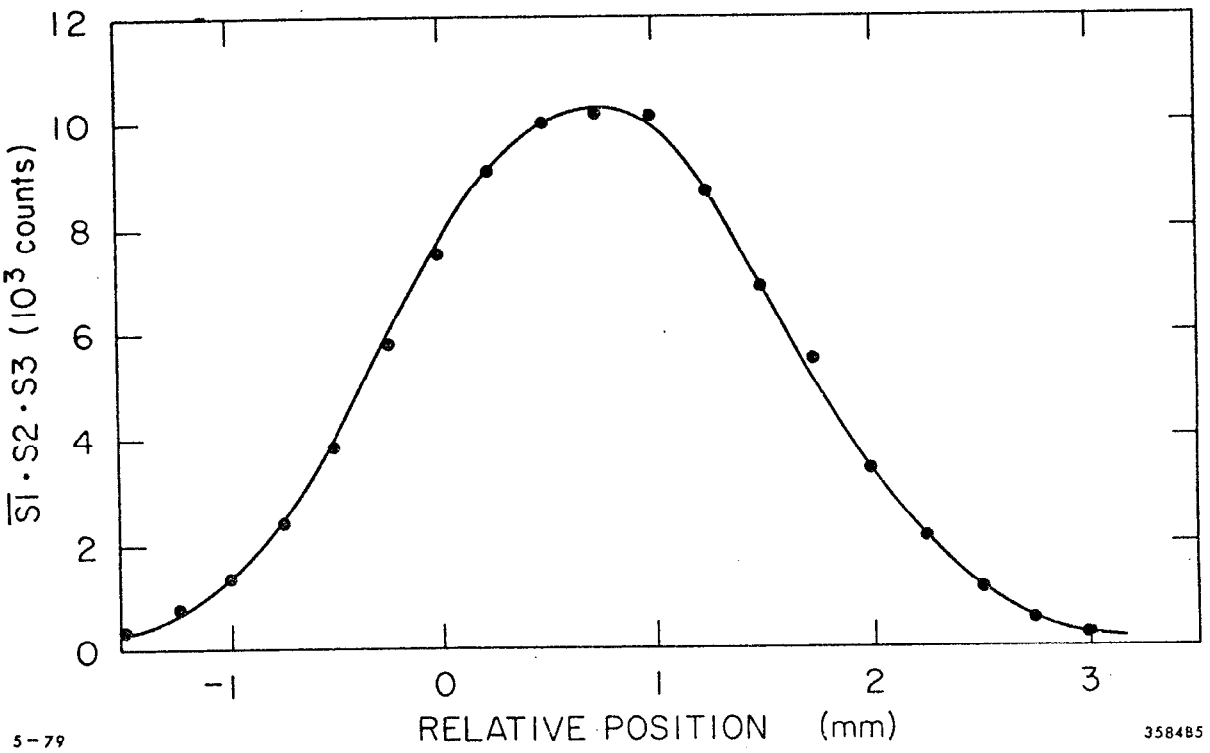
12
10
8
6
4
2
0
$\overline{S1} \cdot S2 \cdot S3$ (10^3 counts)
-1
0
1
2
3
RELATIVE POSITION (mm)
5-79
3584B5

Fig. 8

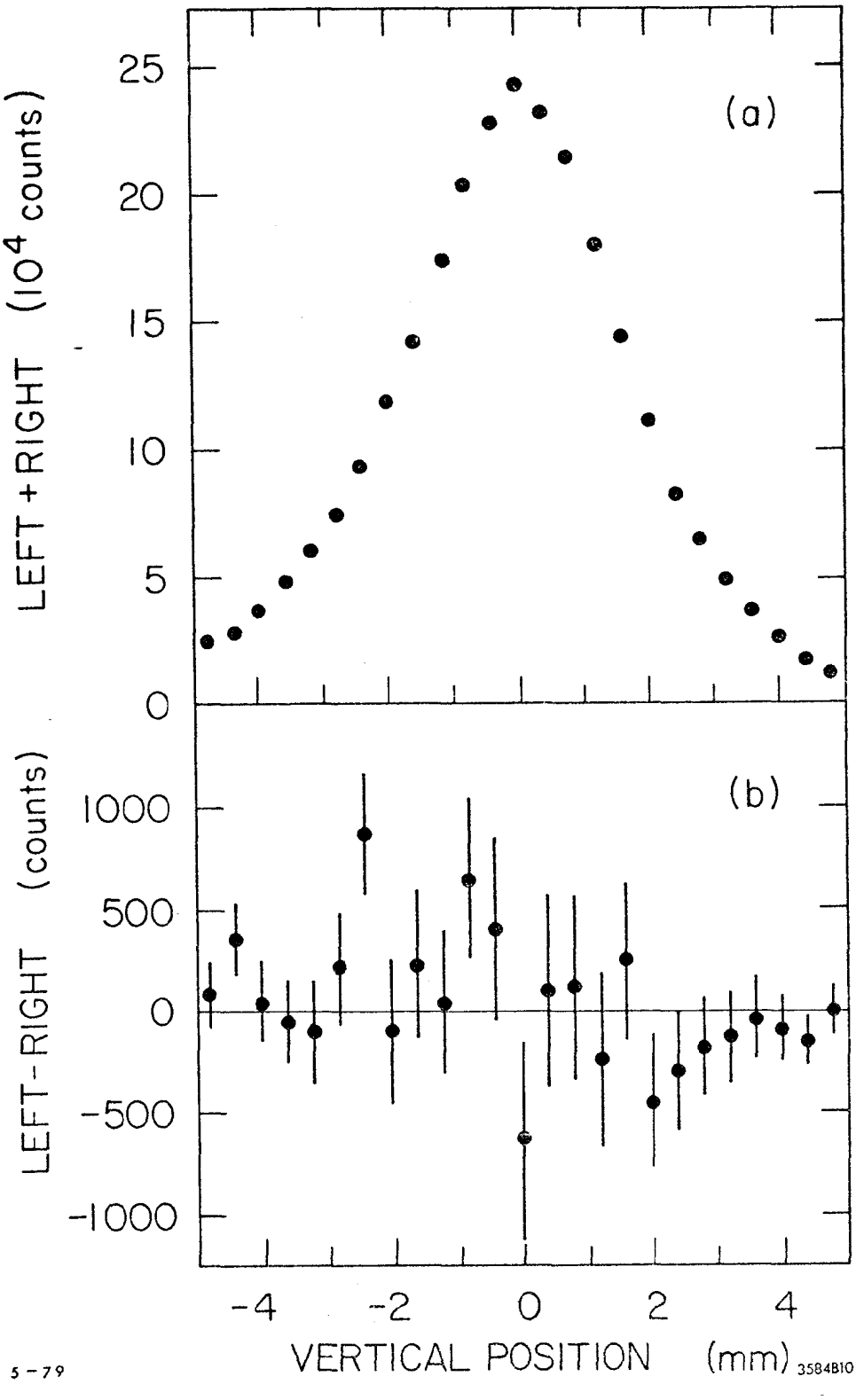
LEFT + RIGHT (10^4 counts)
25
20
15
10
5
0
(a)
LEFT - RIGHT (counts)
1000
500
0
-500
-1000
(b)
-4
-2
0
2
4
VERTICAL POSITION (mm)
5-79
3584B10

Fig. 9

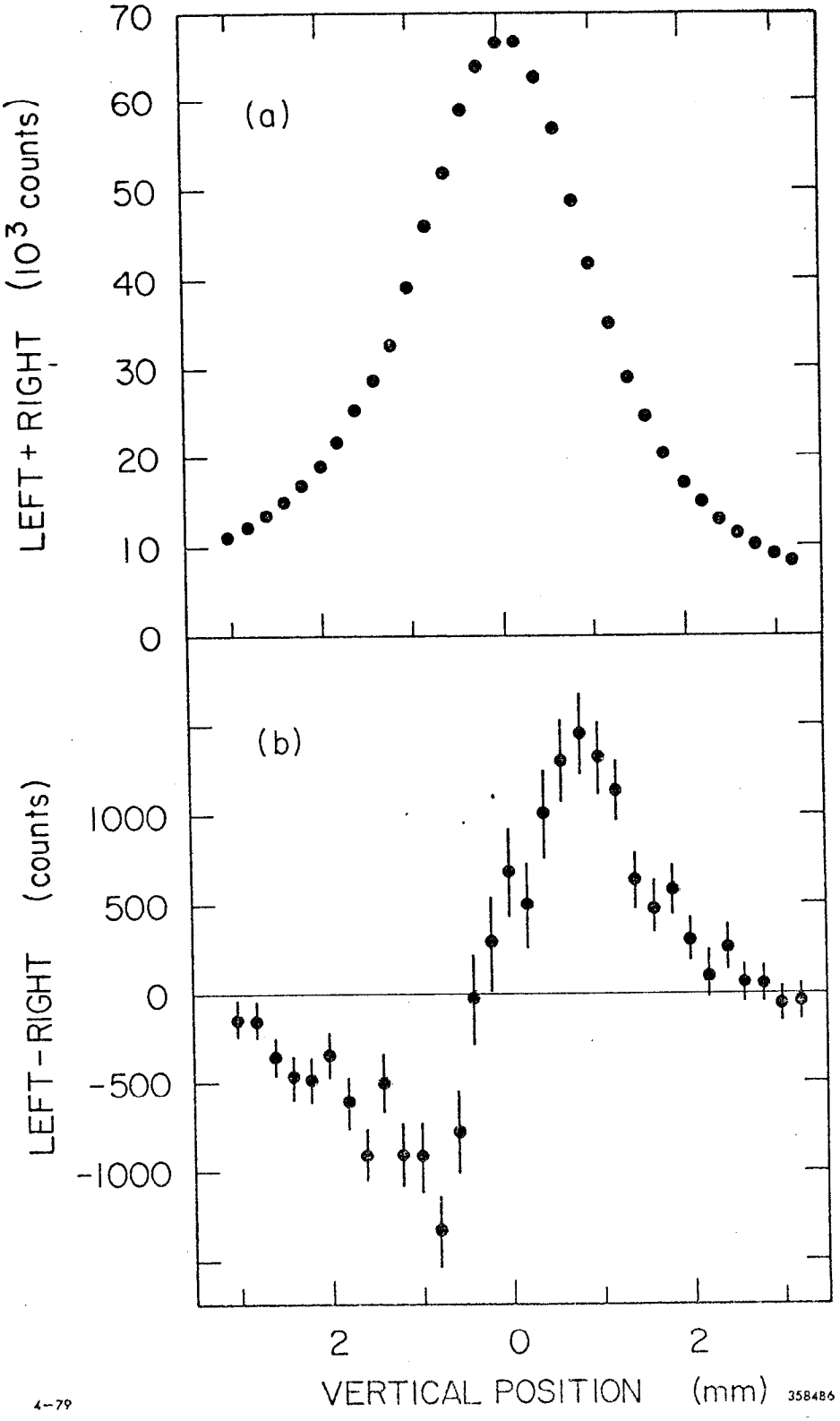
70
60
50
40
30
20
10
0
(a)
LEFT + RIGHT (10³ counts)
(b)
1000
500
0
-500
-1000
LEFT - RIGHT (counts)
2
0
2
VERTICAL POSITION (mm)
4-79
358486

Fig. 10

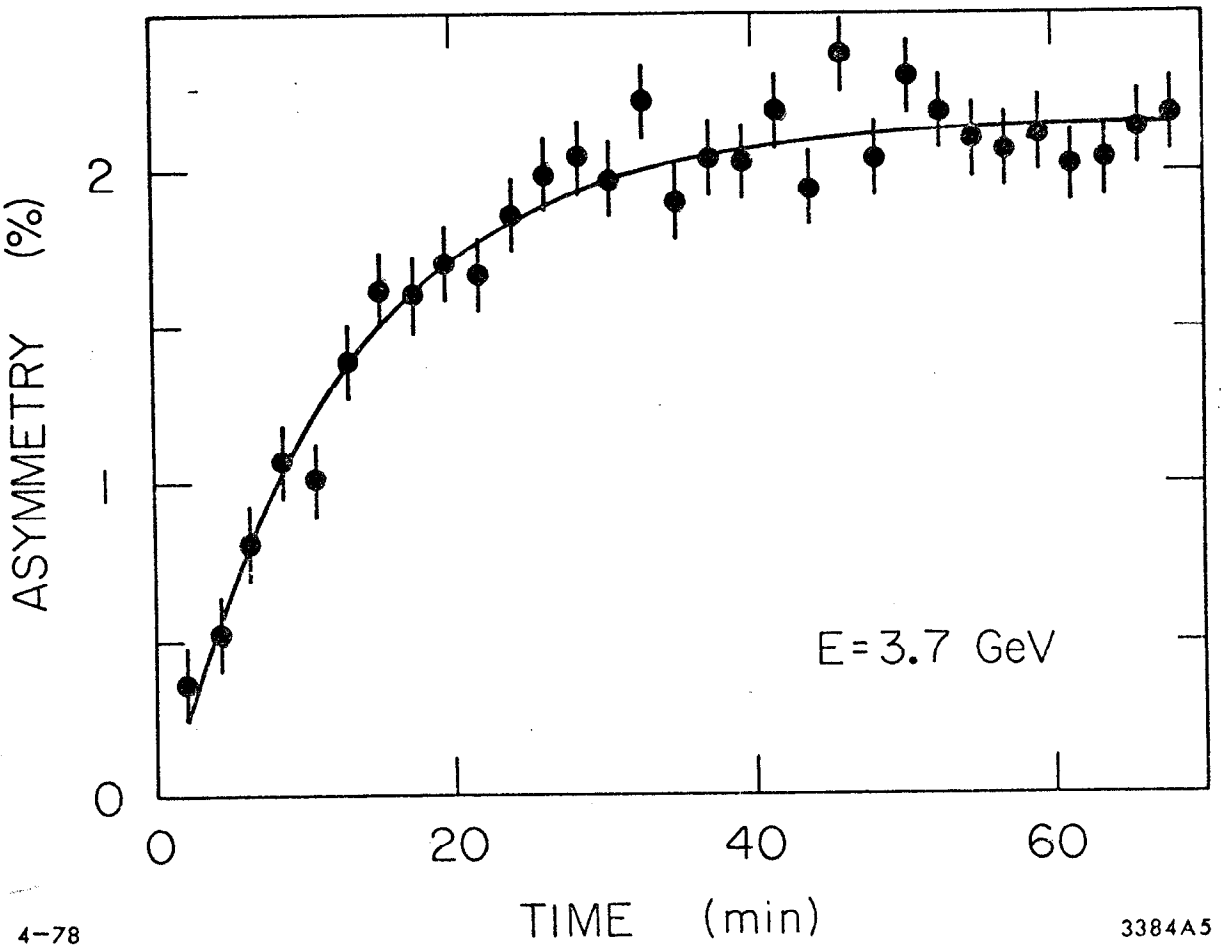

Fig. 11

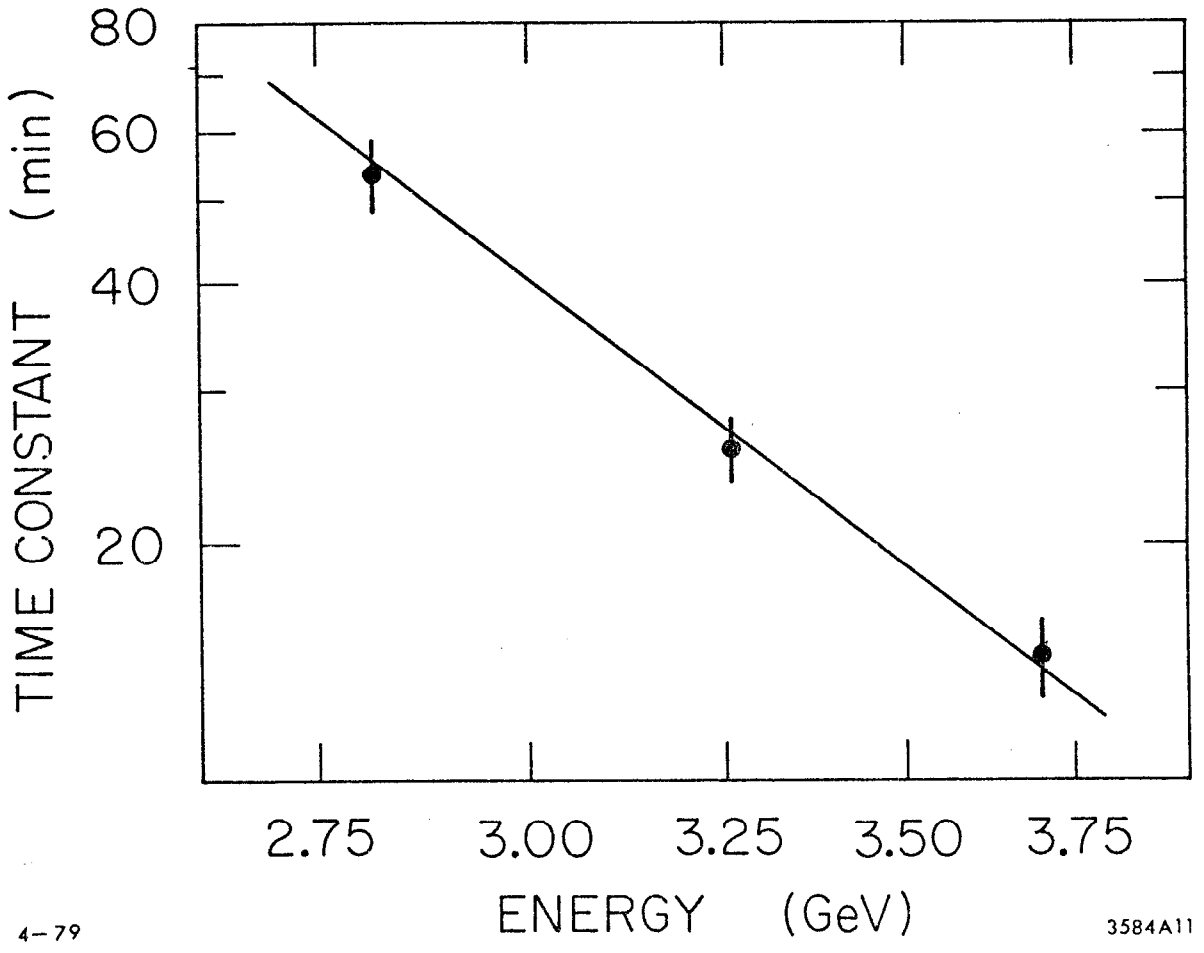
80
60
40
20
TIME CONSTANT (min)
2.75
3.00
3.25
3.50
3.75
ENERGY (GeV)
4-79
3584A11

Fig 12

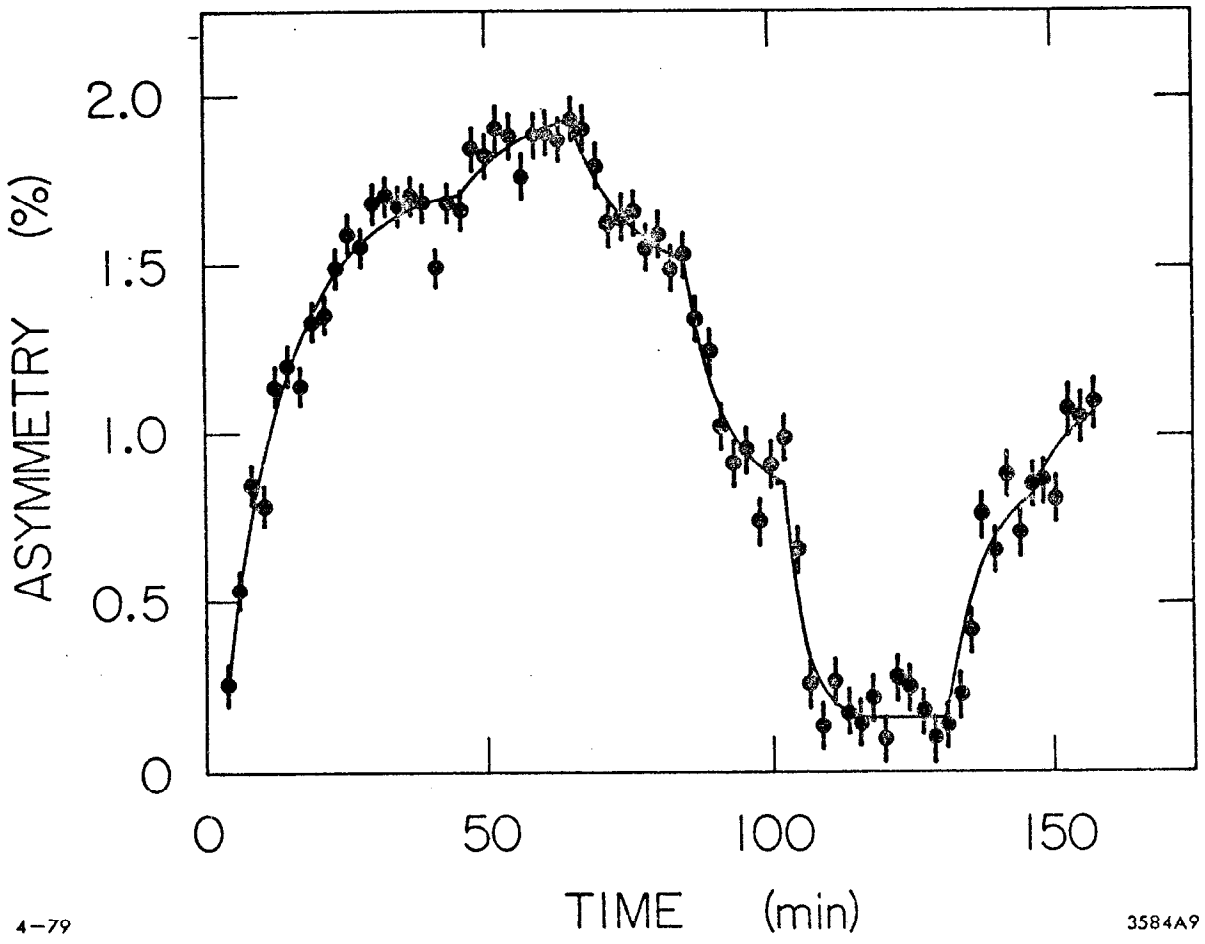

Fig. 13

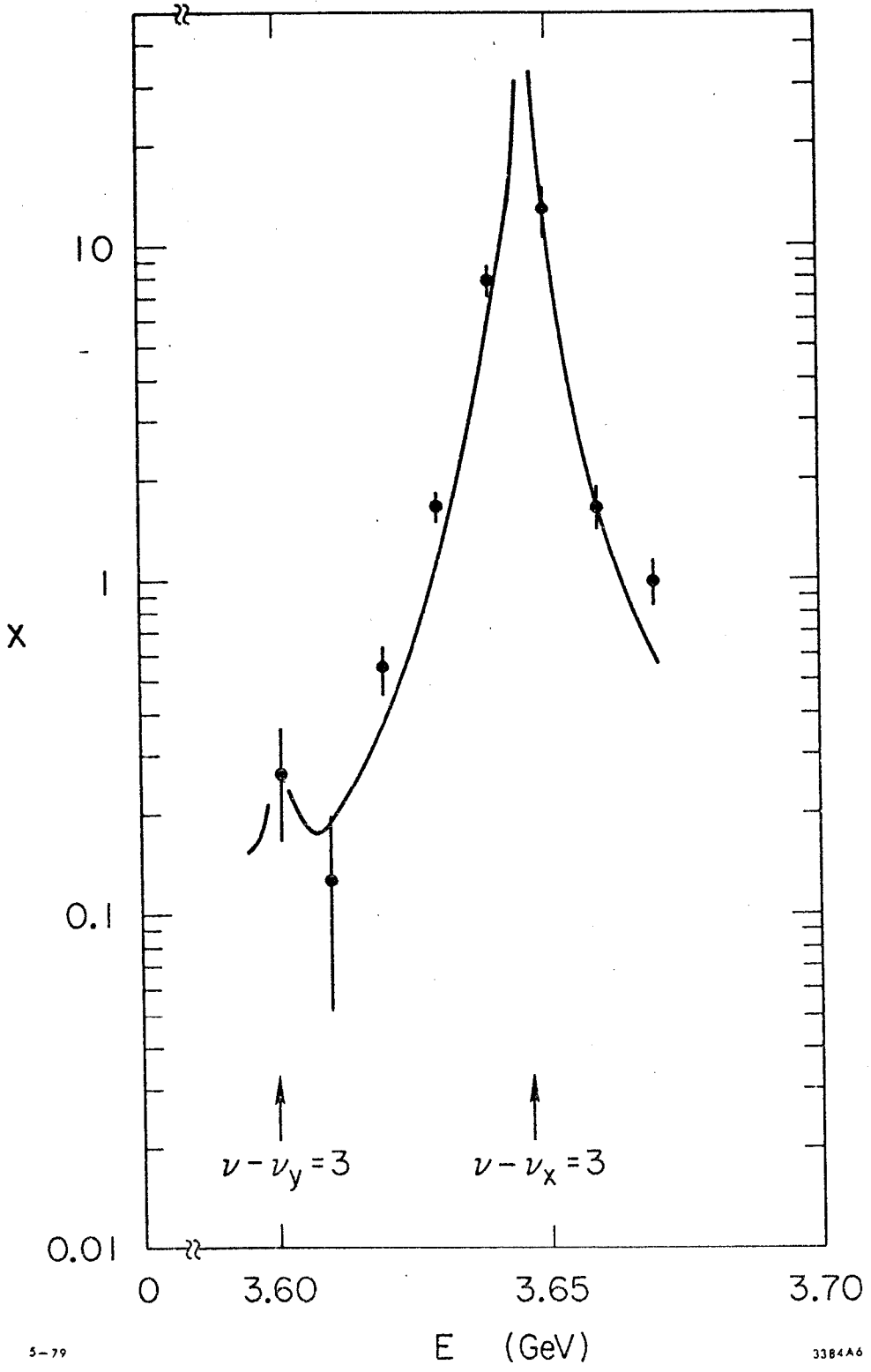

Fig. 14